Structural Engineering and Mechanics, *Vol. 54, No. 4 (2015) 607-622*
DOI: http://dx.doi.org/10.12989/sem.2015.54.4.607

Analytical solution of a contact problem and comparison with the results from FEM

Erdal Öner*[1], Murat Yaylacı[2a] and Ahmet Birinci[3b]

[1]*Department of Civil Engineering, Bayburt University, 69000, Bayburt, Turkey*
[2]*Department of Civil Engineering, Recep Tayyip Erdoğan University, 53100, Rize, Turkey*
[3]*Department of Civil Engineering, Karadeniz Technical University, 61080, Trabzon, Turkey*

(Received June 10, 2014, Revised October 14, 2014, Accepted October 29, 2014)

Abstract. This paper presents a comparative study of analytical method and finite element method (FEM) for analysis of a continuous contact problem. The problem consists of two elastic layers loaded by means of a rigid circular punch and resting on semi-infinite plane. It is assumed that all surfaces are frictionless and only compressive normal tractions can be transmitted through the contact areas. Firstly, analytical solution of the problem is obtained by using theory of elasticity and integral transform techniques. Then, finite element model of the problem is constituted using ANSYS software and the two dimensional analysis of the problem is carried out. The contact stresses under rigid circular punch, the contact areas, normal stresses along the axis of symmetry are obtained for both solutions. The results show that contact stresses and the normal stresses obtained from finite element method (FEM) provide boundary conditions of the problem as well as analytical results. Also, the contact areas obtained from finite element method are very close to results obtained from analytical method; disagree by 0.03-1.61%. Finally, it can be said that there is a good agreement between two methods.

Keywords: contact problem; finite element model; rigid punch; semi-infinite plane; singular integral equation

1. Introduction

Contact problem is a very important subject in both civil and mechanical engineering because of existing the contact between deformable bodies in industry and everyday life. So, the time span of the history shows that these problems continue to be of interest today. The contact problem of two elastic bodies was first considered by Hertz. He neglected all but the leading terms in the equations defining the contacting bodies, and in this way reduced the problem to that of two contacting elliptical paraboloids. In particular he found the solution of the plane contact problem for two parabolic cylinders whose axes were parallel. These results served as the basis of research into contact problems in the theory of elasticity. The solution of these problems was achieved by means of a semi-inverse method, using the expression for the potential for an elliptical disc (Galin

∗Corresponding author, Research Assistant, E-mail: eoner@bayburt.edu.tr
[a]Assistant Professor, E-mail: murat.yaylaci@erdogan.edu.tr
[b]Professor, E-mail: birinci@ktu.edu.tr

http://www.techno-press.org/?journal=sem&subpage=8 ISSN: 1225-4568 (Print), 1598-6217 (Online)

2008). Later, contact problems have been investigated using analytical methods (Alexandrov 1970, Weitsman 1972, Ratwani and Erdogan 1973, Adams 1978, Gecit 1986, Nowell and Hills 1988, Dempsey *et al*. 1990, Cakiroglu *et al*. 2001, Dini and Nowell 2004) and numerical methods (Chan and Tuba 1971, Francavilla and Zienkiewicz 1975, Jing and Liao 1990, Garrido *et al*. 1991, Satish Kumar *et al*. 1996, Garrido and Lorenzana 1998) by several researchers. Beside these studies, the contact pressure distribution was obtained for a square ended rigid punch, pressing normally onto an elastic layer, itself attached to an elastically dissimilar half-plane, under plane deformation by Porter and Hills (2002). The plane problem about surface loading of an elastic layer perfectly bonded to an elastically dissimilar half-plane was carried out by Ma and Korsunsky (2004).

El-Borgi *et al*. (2006) considered the plane problem of a receding contact between an elastic functionally graded layer and a homogeneous half-space when the two bodies were pressed together. Oysu (2007) investigated finite element and boundary element contact stress analysis with remeshing technique. Kahya *et al.* (2007) solved a receding contact problem between an anisotropic elastic layer and an anisotropic elastic half plane, when the two bodies were pressed together by means of a rigid circular stamp. Dag *et al*. (2009) analyzed sliding frictional contact between a rigid punch and a laterally graded elastic medium. The axisymmetric problem of a frictionless double receding contact between a rigid stamp of axisymmetric profile, an elastic functionally graded layer and a homogeneous half space was studied by Rhimi *et al*. (2011). Argatov (2013) carried out contact problem for a thin elastic layer with variable thickness. Long and Wang (2013) investigated effects of surface tension on axisymmetric Hertzian contact problem. The periodic contact problem of the plane theory of elasticity with taking friction, wear and adhesion into account was examined by Soldatenkov (2013). Adibelli *et al*. (2013) solved a receding contact problem for a coated layer and a half-plane loaded by a rigid cylindrical stamp. The receding contact problem of two elastic layers supported by two elastic quarter planes was examined by Yaylaci and Birinci (2013). Kumar and Dasgupta (2013) investigated the mechanics of contact of an inflated spherical non-linear hyperelastic membrane pressed between two rigid plates. Frictional contact problem of a rigid stamp and an elastic layer bonded to a homogeneous substrate was considered by Comez and Erdol (2013). Li *et al*. (2014) studied the fundamental contact solutions of a magneto-electro-elastic half-space indented by a smooth and rigid half-infinite punch. Gun and Gao (2014) presented a quadratic boundary element formulation for continuously non-homogeneous, isotropic and linear elastic functionally graded material contact problems with friction.

In the existing literature, while contact problems have been well studied by analytically and numerically, comparison of two solutions in contact mechanics has not been explored completely. So, the main purpose of this paper is to present a comparative study of the analytical method and the finite element method (FEM) for analysis of a continuous contact problem. The contact stresses under rigid circular punch, the contact areas and normal stresses (σ_x and σ_y) along the axis of symmetry are obtained by using both analytical method and finite element method. Finally, these two solutions are compared with each other.

2. Analytical solution of the problem

2.1 Formulation of the problem

Analytical solution of the problem is obtained using theory of elasticity and integral transform techniques. As shown in Fig. 1, the plane strain problem consists of two infinitely long layers of

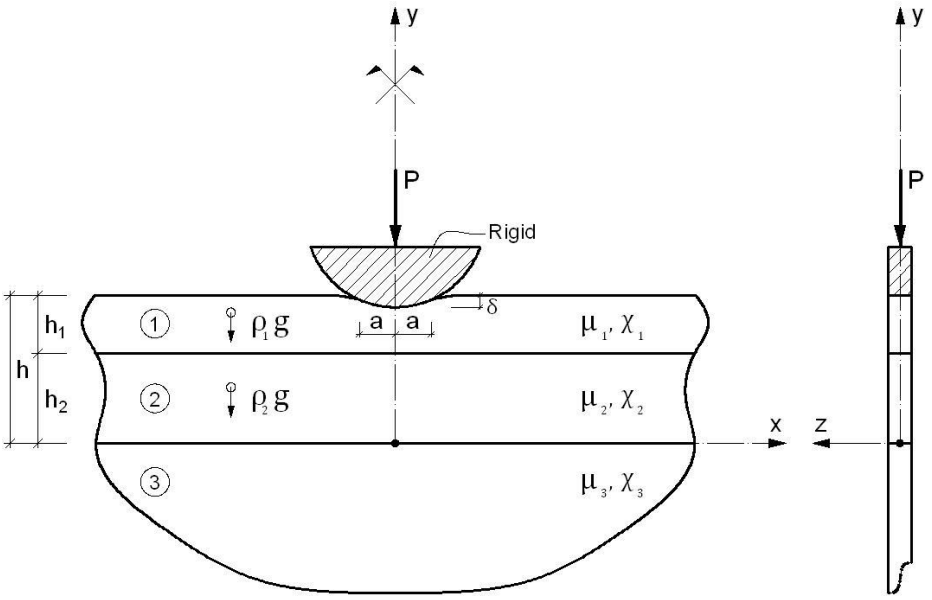

Fig. 1 Geometry and loading condition of the continuous contact problem

thicknesses h_1 and h_2 in smooth contact with each other and semi-infinite plane. Layers and semi-infinite plane are isotropic, homogeneous and linearly elastic. A concentrated load with magnitude P is subjected to upper layer by means of a rigid circular punch. It is assumed that the contact along the interfaces is frictionless, only normal tractions can be transmitted across the contact surfaces, body forces of elastic layers are taken into account, and body force of semi-infinite plane is neglected. Due to symmetry about y-axis, it is sufficient to consider only one-half of the problem geometry. Thickness in z direction is taken to be unit.

For the case which body forces are neglected, the components of stress and displacement for the layers and semi-infinite plane can be written in terms of constant coefficients as (Birinci and Erdol 2001, 2003)

$$u_{ih}(x,y)=\frac{2}{\pi}\int_0^\infty\left\{\left[A_i+B_i y\right]e^{-\alpha y}+\left[C_i+D_i y\right]e^{\alpha y}\right\}\sin(\alpha x)\,d\alpha \tag{1}$$

$$v_{ih}(x,y)=\frac{2}{\pi}\int_0^\infty\left\{\left[A_i+B_i\left(\frac{\chi_i}{\alpha}+y\right)\right]e^{-\alpha y}+\left[-C_i+D_i\left(\frac{\chi_i}{\alpha}-y\right)\right]e^{\alpha y}\right\}\cos(\alpha x)\,d\alpha \tag{2}$$

$$\frac{1}{2\mu_i}\sigma_{ixh}(x,y)=\frac{2}{\pi}\int_0^\infty\left\{\left[\alpha(A_i+B_i y)-\left(\frac{3-\chi_i}{2}\right)B_i\right]e^{-\alpha y}+\left[\alpha(C_i+D_i y)+\left(\frac{3-\chi_i}{2}\right)D_i\right]e^{\alpha y}\right\}\cos(\alpha x)\,d\alpha \tag{3}$$

$$\frac{1}{2\mu_i}\sigma_{iyh}(x,y)=\frac{2}{\pi}\int_0^\infty\left\{-\left[\alpha(A_i+B_i y)+\left(\frac{1+\chi_i}{2}\right)B_i\right]e^{-\alpha y}+\left[-\alpha(C_i+D_i y)+\left(\frac{1+\chi_i}{2}\right)D_i\right]e^{\alpha y}\right\}\cos(\alpha x)\,d\alpha \tag{4}$$

$$\frac{1}{2\mu_i}\tau_{ixyh}(x,y)=\frac{2}{\pi}\int_0^\infty\left\{-\left[\alpha(A_i+B_i y)+\left(\frac{\chi_i-1}{2}\right)B_i\right]e^{-\alpha y}+\left[\alpha(C_i+D_i y)-\left(\frac{\chi_i-1}{2}\right)D_i\right]e^{\alpha y}\right\}\sin(\alpha x)\,d\alpha \tag{5}$$

where i=1,2

$$u_{3h}(x,y)=\frac{2}{\pi}\int_0^{\infty}\left\{\left[C_3+D_3y\right]e^{\alpha y}\right\}\sin(\alpha x)d\alpha \tag{6}$$

$$v_{3h}(x,y)=\frac{2}{\pi}\int_0^{\infty}\left\{\left[-C_3+D_3\left(\frac{\chi_3}{\alpha}-y\right)\right]e^{\alpha y}\right\}\cos(\alpha x)d\alpha \tag{7}$$

$$\frac{1}{2\mu_3}\sigma_{3xh}(x,y)=\frac{2}{\pi}\int_0^{\infty}\left\{\left[\alpha\left(C_3+D_3y\right)+\left(\frac{3-\chi_3}{2}\right)D_3\right]e^{\alpha y}\right\}\cos(\alpha x)d\alpha \tag{8}$$

$$\frac{1}{2\mu_3}\sigma_{3yh}(x,y)=\frac{2}{\pi}\int_0^{\infty}\left\{\left[-\alpha\left(C_3+D_3y\right)+\left(\frac{1+\chi_3}{2}\right)D_3\right]e^{\alpha y}\right\}\cos(\alpha x)d\alpha \tag{9}$$

$$\frac{1}{2\mu_3}\tau_{3xyh}(x,y)=\frac{2}{\pi}\int_0^{\infty}\left\{\left[\alpha\left(C_3+D_3y\right)-\left(\frac{\chi_3-1}{2}\right)D_3\right]e^{\alpha y}\right\}\sin(\alpha x)d\alpha \tag{10}$$

where $u=u(x,y)$ and $v=v(x,y)$ are the x- and y- components of the displacement vector, respectively. χ_i is an elastic constant and $\chi_i=(3-4\nu_i)$ for plane strain, μ_i is shear modulus, ν_i is Poisson's ratio (i=1,…,3). The subscripts 1, 2 and 3 refer to the upper layer, lower layer and semi-infinite plane, respectively. Subscript h indicates the case without body forces. A_i, B_i, C_i, D_i (i=1, 2) and C_3, D_3 are unknown coefficients which will be determined from boundary conditions of the problem.

The components of normal stresses for the case which body forces of the layers existing may be obtained as

$$\sigma_{1xp}(y)=\frac{3-\chi_1}{1+\chi_1}\frac{\rho_1 g}{2}\left(2y-h-h_2\right)\quad h_2\le y\le h \tag{11}$$

$$\sigma_{1yp}(y)=\rho_1 g(y-h)\qquad h_2\le y\le h \tag{12}$$

$$\sigma_{2xp}(y)=\frac{3-\chi_2}{1+\chi_2}\frac{\rho_2 g}{2}\left(2y-h_2\right)\qquad 0\le y\le h_2 \tag{13}$$

$$\sigma_{2yp}(y)=-\rho_1 g h_1+\rho_2 g(y-h_2)\qquad 0\le y\le h_2 \tag{14}$$

$$\sigma_{3yp}(y)=-(\rho_1 g h_1+\rho_2 g h_2)\qquad y\le 0 \tag{15}$$

$$\sigma_{3xp}=0 \tag{16}$$

where $\rho_1 g$ and $\rho_2 g$ are body forces acting in vertically in the layers. Subscript p indicates the case which body forces of layers exist. The total normal stress expressions will be the superposition of two cases for which body forces of the layers are taken into account and body forces of the layers are neglected as

$$\sigma_{ix}(x,y)=\sigma_{ixp}(y)+\sigma_{ixh}(x,y) \tag{17}$$

$$\sigma_{iy}(x,y)=\sigma_{iyp}(y)+\sigma_{iyh}(x,y)\qquad (i=1,\,2,\,3) \tag{18}$$

2.2 Boundary conditions of the problem and solution of the singular integral equation

The plane contact problem outlined above as shown in Fig. 1 must be solved under the following boundary conditions

$$\tau_{1xy}(x,h)=0, \qquad (0\le x<\infty) \tag{19}$$

$$\sigma_{1y}(x,h)=\begin{cases}-p(x)\ ; & (0\le x<a)\\ 0\ ; & (a\le x<\infty)\end{cases} \tag{20}$$

$$\tau_{1xy}(x,h_2)=0\ ; \qquad (0\le x<\infty) \tag{21}$$

$$\tau_{2xy}(x,h_2)=0\ ; \qquad (0\le x<\infty) \tag{22}$$

$$\sigma_{1y}(x,h_2)=\sigma_{2y}(x,h_2)\ ; \qquad (0\le x<\infty) \tag{23}$$

$$\frac{\partial}{\partial x}\left[v_1(x,h_2)-v_2(x,h_2)\right]=0\ ; \qquad (0\le x<\infty) \tag{24}$$

$$\tau_{2xy}(x,0)=0\ ; \qquad (0\le x<\infty) \tag{25}$$

$$\tau_{3xy}(x,0)=0\ ; \qquad (0\le x<\infty) \tag{26}$$

$$\sigma_{2y}(x,0)=\sigma_{3y}(x,0)\ ; \qquad (0\le x<\infty) \tag{27}$$

$$\frac{\partial}{\partial x}\left[v_2(x,0)-v_3(x,0)\right]=0\ ; \qquad (0\le x<\infty) \tag{28}$$

$$\frac{\partial}{\partial x}\left[v_1(x,h)\right]=f(x)\ ; \qquad (0\le x<a) \tag{29}$$

where **a** is the half-width of the contact area between rigid circular punch and the upper layer, $p(x)$ is the unknown contact stress under the rigid circular punch, $f(x)$ is the derivative of the function $F(x)$ which characterizes profile of the rigid punch. In case of circular punch, $f(x)$ can be obtained as

$$F(x)=h-\delta-\left[\left(R^2-x^2\right)^{1/2}-R\right] \tag{30}$$

$$f(x)=\frac{d}{dx}\left[F(x)\right]=-\frac{x}{\left(R^2-x^2\right)^{1/2}} \tag{31}$$

where δ is the maximum displacement which occurs on the layer under the punch on the axis of symmetry (x=0), R is the radius of rigid circular punch. Applying the boundary conditions (19-28) to the stress and displacement expressions, A_i, B_i, C_i, D_i (i=1, 2) and C_3, D_3 coefficients can be determined in terms of the unknown contact stress $p(x)$, and by substituting these coefficients into Eq. (29), after some routine manipulations and using the symmetry condition $p(x)=p(-x)$, one may obtain the following singular integral equation for $p(x)$.

$$\int_{-a}^{a}\left[\frac{1}{t-x}+k(x,t)\right]p(t)dt=-\frac{4\pi\mu_1}{1+\chi_1}f(x) \qquad (-a<x<a) \tag{32}$$

where the kernel $k(x,t)$ is given by (A.1) in Appendix. The equilibrium condition of the problem may be expressed as

$$\int_{-a}^{a}p(t)dt=P \tag{33}$$

In order to simplify the numerical solution of the singular integral equation, the following dimensionless quantities can be defined for normalizing the intervals $(-a, +a)$ to $(-1, +1)$

$$x=as, \quad t=ar, \quad \phi(r)=\frac{p(ar)}{P/h}, \quad M(s)=\frac{m(as)}{P/h}, \quad m(as)=-\frac{4\pi\mu_1}{1+\chi_1}f(as) \tag{34}$$

Substituting from Eq. (34), Eqs. (32)-(33) can be obtained as

$$\int_{-1}^{1}\left[\frac{1}{r-s}+N(s,r)\right]\phi(r)dr=M(s) \qquad (-1<s<1) \quad , N(s,r) = ak(as,ar) \tag{35}$$

$$\frac{a}{h}\int_{-1}^{1}\phi(r)dr=1 \tag{36}$$

Due to the smooth contact at the end point a, the unknown function $p(t)$ is zero. Therefore, the index of integral equation in (35) is -1 (Erdogan and Gupta 1972). Writing the solution

$$\phi(r)=g(r)(1-r^2)^{1/2}, \qquad (-1<r<1) \tag{37}$$

and using the appropriate Gauss-Chebyshev integration formula, Eqs. (35) and (36) may be reduced to the following forms.

$$\begin{aligned}&\sum_{i=1}^{n}(1-r_i^2)\left[\frac{1}{r_i-s_j}+N(s_j,r_i)\right]g(r_i)=\frac{n+1}{\pi}M(s_j), \qquad (j=1,...,n+1)\\ &\frac{a}{h}\sum_{i=1}^{n}(1-r_i^2)g(r_i)=\frac{n+1}{\pi}\end{aligned} \tag{38}$$

where

$$r_i=\cos\left(\frac{i\pi}{n+1}\right), \qquad (i=1,...,n) \tag{39}$$

$$s_j=\cos\left(\frac{2j-1}{n+1}\frac{\pi}{2}\right), \qquad (j=1,...,n+1) \tag{40}$$

The extra equation in (38) corresponds to the consistency condition of the original integral equation in (35). In this case, the $(n+1/2)^{th}$ equation in (38) satisfied automatically. Hence, the equations in (38) constitute a system of $n+1$ equations for $n+1$ unknowns. Note that the system is

highly non-linear in **a** and an interpolation scheme is required to determine this unknown. Solving this system of equations and using Eq. (37), $\phi(r)$ normalized contact stress distribution and half-width of contact area (**a**) are obtained. By using (37), substituting the results into Eqs. (17) and (18) and using Gauss integration formula, the dimensionless normal stresses along the axis of symmetry $\sigma_x(0, y)/(P/h)$ and $\sigma_y(0, y)/(P/h)$ are determined.

3. Modelling with finite elements in ANSYS

Contact is a phenomenon that occurs in many engineering applications. Additionally, the analysis on contact parameters and stresses is important to engineering design. Contact problems present significant difficulty, contacting surfaces change unpredictably.

With the development of computer technology, attention in solution of contact problems has shifted from traditional analytic solution towards finite element analysis (FEA). The FEM is a numerical method effectively used to resolve complex engineering problems. The FEM versatility lies in its ability to model arbitrary shaped structures, work with complex materials, and apply various types of loading and boundary conditions. The method can easily be adapted to different sets of constitutive equations, which makes it particularly attractive for coupled physics simulation.

The main problem of the FEM in the contact problems is to compute the fields of contact area and contact pressure. The structure to be analyzed is discretized with a number of elements and then assembled at nodes. In FEM, the function in question is piecewise approximated by means of polynomials over every element and expressed in terms of nodal values. The elements of different type and shape with complex loads and boundary conditions can be used simultaneously. In the structural analysis, the degrees of freedom are defined as nodal displacements. The equations for every element are assembled as

$$[D]\{u\} = \{F\} \tag{41}$$

where $[D]$ is the global stiffness matrix, $\{u\}$ the structural nodal displacement vector and $\{F\}$ is the vector of structural nodal loads. This equation system can be solved for $\{u\}$ (Zhang and Meng 2006).

In this paper we shall study a very simple case using the well-known finite element software ANSYS (2008). The geometrical model is created with standard tools in the ANSYS software. Plain strain problems were modelled as the two dimensional (2D) instead of the three dimensional (3D) in the literature because of obtaining very close results to each other in both cases (Etsion *et al.* 2005, Brizmer *et al.* 2006, Rončević and Siminiati 2010). Therefore, axisymmetric 2D model has been used in this study. The model shown in Fig. 2 had a finite element mesh that consisted of 41526 eight-node triangular elements of type PLANE183 comprising a total of 82896 nodes. PLANE183 is defined by eight nodes having two degrees of freedom at each node: translations in the nodal x and y directions. In addition this element has the capability, plasticity, elasticity, creep, swelling, stress stiffening, large deflection, and large strain capabilities. 2-D finite contact (CONTA172) and target (TARGE169) elements have been used as a surface-to-surface 5045 contact pair. CONTA172 is used to represent that of the mechanical contact analysis. The target surface, defined by TARGE169, was therefore used to represent 2-D "target" surfaces for the associated contact elements CONTA172. Frictionless surface-to-surface contact elements are used to model the interaction between the lower surface and the top surface of the layers and semi-

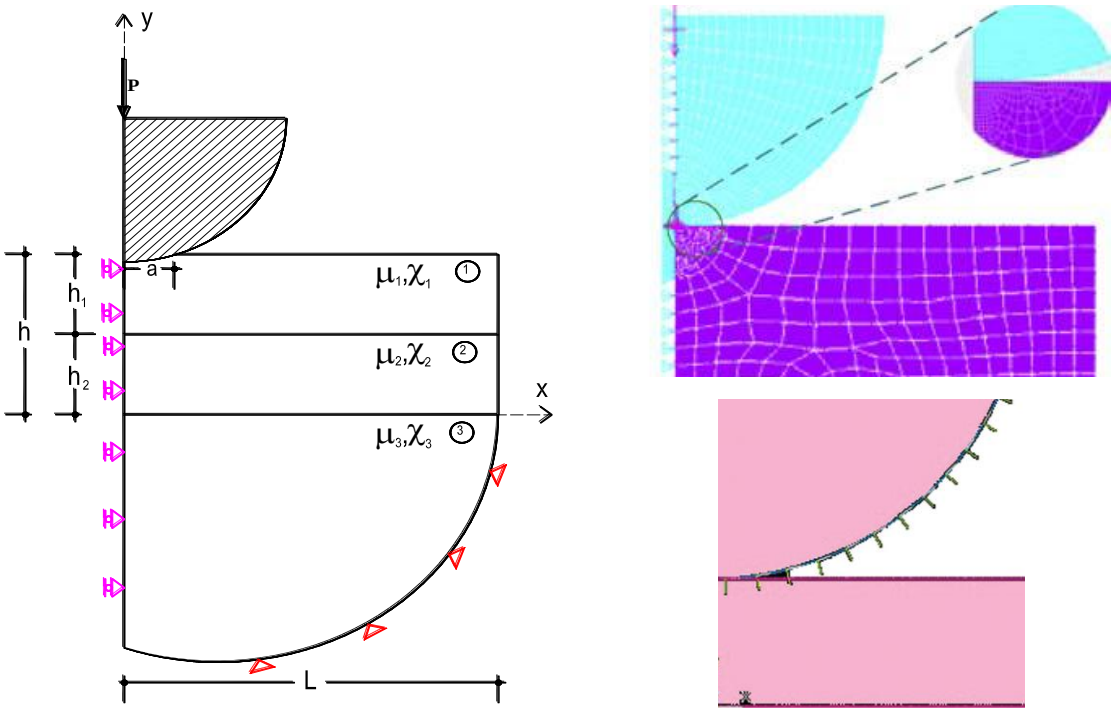

Fig. 2 Schematic model of the contact problem (symmetric finite element model)

infinite plane. The layers and semi-infinite plane are assumed elastic and isotropic. In the analyses, geometric properties are taken as L=1 m (length of the layer in x direction), h_1=h_2=10 cm (thicknesses of the layers in y direction) and R=0.5 m (radius of the punch) and material properties are taken as E_1=25000 MPa, ν_1=0,25, E_2=50000 MPa, ν_2=0,25 and E_3=100000 MPa, ν_3=0,25. Other parameters are chosen such that R/h, $\mu_1/(P/h)$, μ_2/μ_1, μ_3/μ_2 ratios are compatible with analytical values. Several numerical solution methods have been proposed to solve the variational equation of the elastic contact problem, including penalty method, augmented Lagrangian method, Lagrange multiplier method and augmented Lagrangian multiplier method. These methods, incorporated to general finite element analysis (FEA) technology, are applied to solve the contact problem that involves complex geometry shapes. In the penalty method, the accuracy of the solution depends on the choice of the penalty parameter. Too small a penalty parameter may cause unacceptable error in the solution. Also, the penalty method suffers from ill conditioning as the penalty parameter becomes large. The augmented Lagrangian method is an iterative series of penalty methods. The contact tractions (pressure and frictional stresses) are augmented during equilibrium iterations so that the final penetration is smaller than the allowable tolerance. Compared to the penalty method, the augmented Lagrangian method usually leads to better conditioning and is less sensitive to the magnitude of the contact stiffness. The Lagrange multiplier method introduces new unknowns for each constraint. Therefore, it always increases the dimension of the system equations to be solved. For large-scale problems where the contact surface consists of a large number of nodes, the number of unknowns introduced by the Lagrange multiplier method is also large. This increases the CPU time to solve the problem. For the augmented Lagrangian multiplier method, both penalty parameters and Lagrangian multipliers are

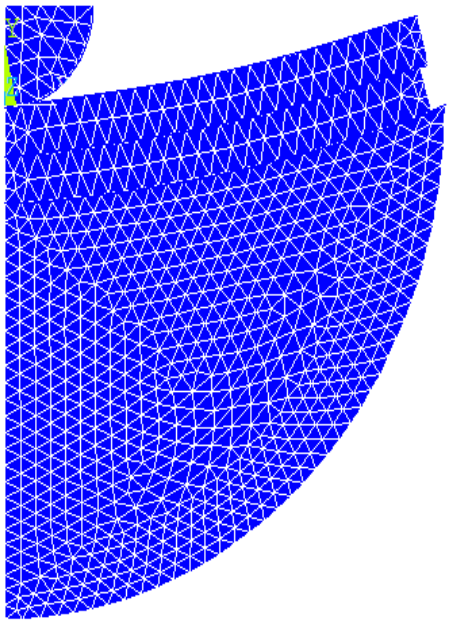

Fig. 3 Deformation shape after the analysis

Table 1 Variation of half-width of the contact area (a/h) with (R/h) ($\mu_1/(P/h)$=100, h_2/h_1=1, μ_2/μ_1=2, μ_3/μ_2=2)

PARAMETER	R/h=50	R/h=100	R/h=550	R/h=500
	a/h	a/h	a/h	a/h
Analytical	0.4762	0.6541	0.9747	1.3043
ANSYS	0.475	0.65	0.975	1.3
Difference (%)	0.25	0.63	0.03	0.33

Table 2 Variation of half-width of the contact area (a/h) with $\mu_1/(P/h)$. (R/h=500, h_2/h_1=1, μ_2/μ_1=2, μ_3/μ_2=2)

PARAMETER	$\mu_1/(P/h)=100$	$\mu_1/(P/h)=250$	$\mu_1/(P/h)=500$	$\mu_1/(P/h)=1000$
	a/h	a/h	a/h	a/h
Analytical	1.3043	0.8861	0.6541	0.4762
ANSYS	1.3	0.8875	0.65	0.475
Difference (%)	0.33	0.16	0.63	0.25

applied, and penetration is admissible but controlled by allowable tolerance (Liao and Wang 2007). In this study, Aughment Lagrangian method is used for contact modelling and the deformation shape after analysis is shown in Fig. 3.

4. Numerical results and discussion

The variations of contact stresses under rigid circular punch, the contact areas, normal stresses (σ_x and σ_y) along the axis of symmetry are obtained for various dimensionless quantities such as

Table 3 Variation of half-width of the contact area (a/h) with (μ_2/μ_1). (R/h=500, $\mu_1/(P/h)$=100, h_2/h_1=1, μ_3/μ_2=2)

PARAMETER	$\mu_2/\mu_1 = 0.5$	$\mu_2/\mu_1 = 1$	$\mu_2/\mu_1 = 2$	$\mu_2/\mu_1 = 4$
	a/h	a/h	a/h	a/h
Analytical	0.8687	0.7336	0.6541	0.6098
ANSYS	0.875	0.725	0.65	0.6
Difference (%)	0.73	1.17	0.63	1.61

Table 4 Variation of half-width of the contact area (a/h) with (μ_3/μ_2). R/h=500, $\mu_1/(P/h)$=100, h_2/h_1=1, μ_2/μ_1=2)

PARAMETER	$\mu_3/\mu_2 = 0.5$	$\mu_3/\mu_2 = 1$	$\mu_3/\mu_2 = 2$	$\mu_3/\mu_2 = 4$
	a/h	a/h	a/h	a/h
Analytical	0.7585	0.6906	0.6541	0.6347
ANSYS	0.75	0.6875	0.65	0.6375
Difference (%)	1.12	0.45	0.63	0.44

R/h, $\mu_1/(P/h)$, μ_2/μ_1, μ_3/μ_2 using both analytical method and finite element method (FEM). Analytical results are verified by comparison with FEM results. ($\chi_1=\chi_2=\chi_3=2$)

In Tables 1-4, variations of half-width of the contact area (a/h) depending on geometry and material properties are given. The variation of half-width of the contact area (a/h) with radius of circular punch (R/h) is shown in Table 1. It appears that, with increasing radius of punch, half-width of the contact area (a/h) increases. This is an expected result. Table 2 presents variation of half-width of the contact area (a/h) with load ratio $\mu_1/(P/h)$. When Table 2 is examined, it can be seen that half-width of the contact area (a/h) decreases with increasing load ratio $\mu_1/(P/h)$. Table 3 shows variation of half-width of the contact area (a/h) with ratio of the elastic constants (μ_2/μ_1).

In the event of decreasing ratio of the elastic constants (μ_2/μ_1), it is indicated that (a/h) increases. Variation of half-width of the contact area (a/h) with ratio of the elastic constants (μ_3/μ_2) is given in Table 4. It may be observed clearly in the Table 4 that as (μ_3/μ_2) increases, half-width of the contact area (a/h) decreases. It can be seen from all tables that contact areas obtained from ANSYS software are very close to analytical results and a good agreement between two method is observed during this comparison, disagree by 0.03-1.61%.

The contact stress distributions for various values of R/h, $\mu_1/(P/h)$, μ_2/μ_1, μ_3/μ_2 are given in Figs. 4-7. The contact stress distribution for various values of R/h is shown in Fig. 4. As seen in Fig. 4, with increasing radius of punch, the contact stress distribution $p(x)/(P/h)$ decreases. Fig. 5 shows the variation of $p(x)/(P/h)$with load ratio $\mu_1/(P/h)$. In the event of increasing load ratio, it is indicated that contact stress distribution under the punch increases. The contact stress distributions for various values of (μ_2/μ_1) and (μ_3/μ_2) are given in Figs. 6-7. As seen in Figs. 6-7, the contact stress distribution $p(x)/(P/h)$ increases with increasing of (μ_2/μ_1) and (μ_3/μ_2). Furthermore, all figures show that contact stress distribution under rigid punch is symmetrical, its maximum value occurs at x=0 and its value is zero at the end points of contact ($-a$, $+a$). When the analytical and FEM results are compared with each other, it can be clearly seen that there is a good agreement between two methods.

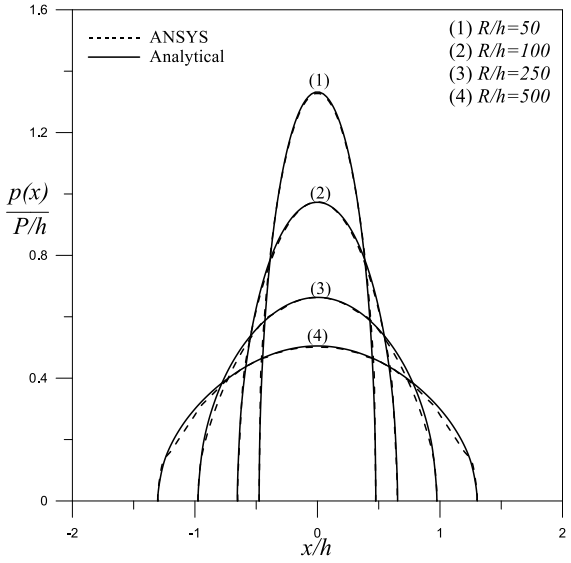

($\mu_1/(P/h)$=100, h_2/h_1=1, $\mu_2/\mu_1=\mu_3/\mu_2$=2

Fig. 4 The effect of (R/h) on dimensionless contact stress distribution under the punch

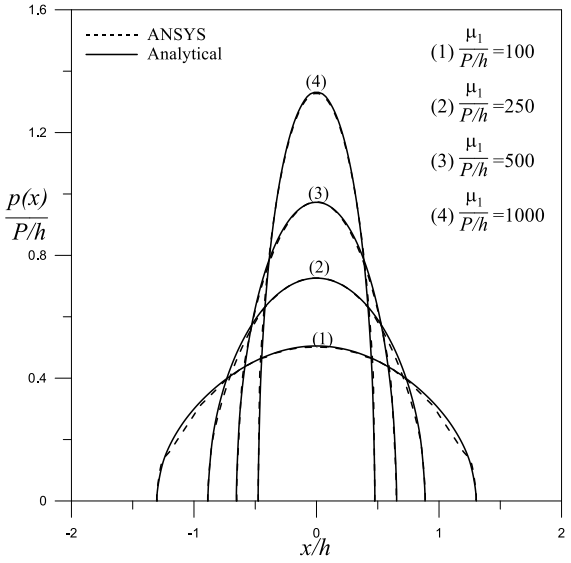

(R/h)=500, h_2/h_1=1, $\mu_2/\mu_1=\mu_3/\mu_2$=2

Fig. 5 The effect of $\mu_1/(P/h)$ on dimensionless contact stress distribution under the punch

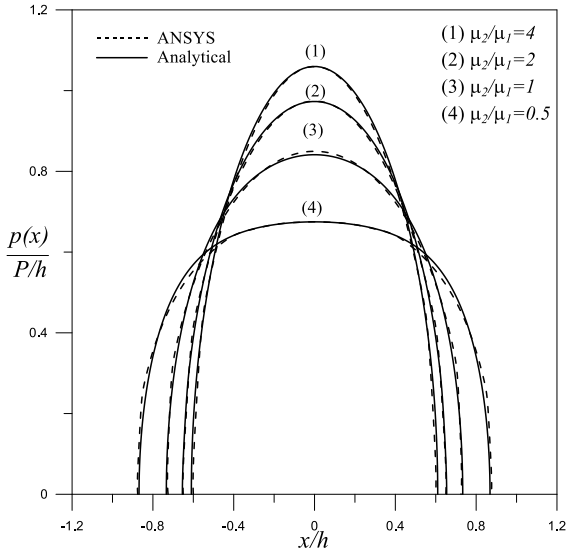

(R/h)=500, $\mu_1/(P/h)$=100, h_2/h_1=1, μ_3/μ_2=2

Fig. 6 The effect of (μ_2/μ_1) on dimensionless contact stress distribution under the punch

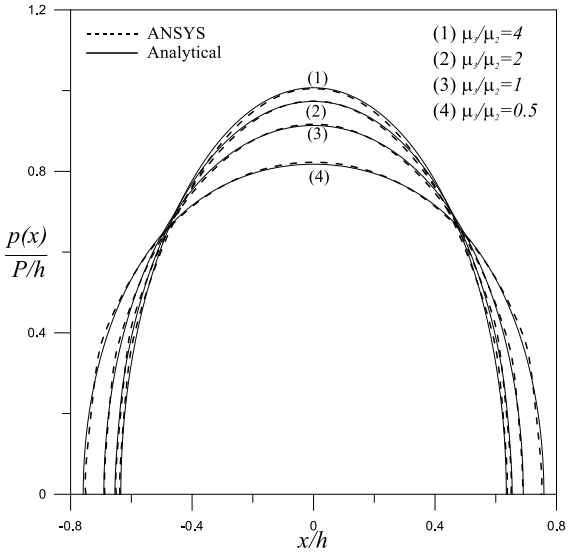

(R/h)=500, $\mu_1/(P/h)$=100, h_2/h_1=1, μ_2/μ_1=2

Fig. 7 The effect of (μ_3/μ_2) on dimensionless contact stress distribution under the punch

Figs. 8-9 show the dimensionless normal stress distributions $\sigma_x(0,y)/(P/h)$ and $\sigma_y(0,y)/(P/h)$ along the axis of symmetry for various value of R/h. As it can be observed in the figures that $\sigma_x(0,y)/(P/h)$ and $\sigma_y(0,y)/(P/h)$ decrease with increasing R/h. The dimensionless normal stress distributions $\sigma_x(0,y)/(P/h)$ and $\sigma_y(0,y)/(P/h)$ along the axis of symmetry for various value of

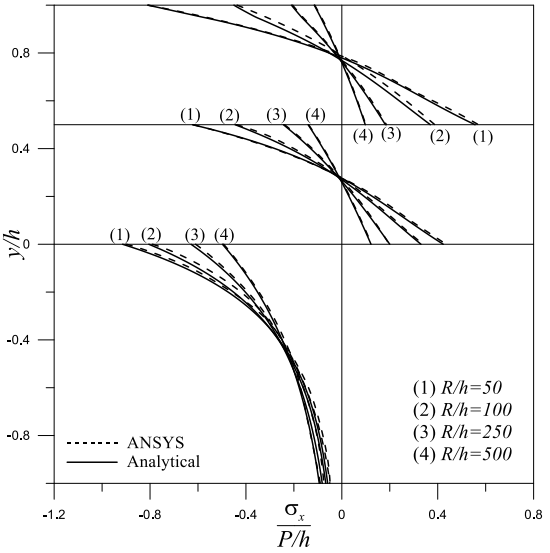

$\mu_1/(P/h)$=100, h_2/h_1=1, μ_2/μ_1= μ_3/μ_2=2, $\rho_1 g h h_1/P$=0.2, ρ_2/ρ_1=1

Fig. 8 The dimensionless normal stress distribution $\sigma_x(0,y)/(P/h)$ along the axis of symmetry for (R/h)

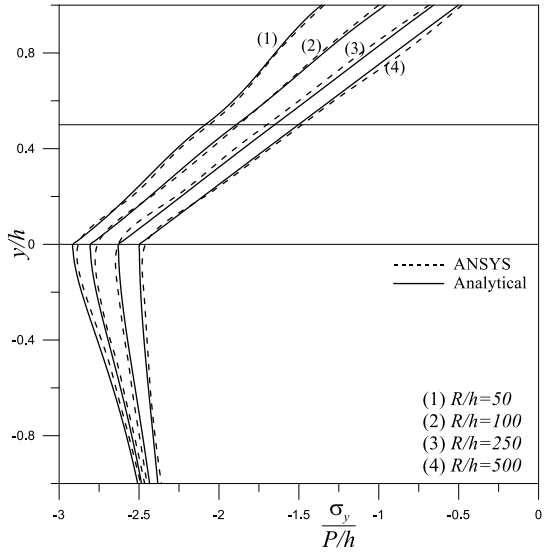

$\mu_1/(P/h)$=100, h_2/h_1=1, μ_2/μ_1= μ_3/μ_2=2, $\rho_1 g h h_1/P$=1, ρ_2/ρ_1=1

Fig. 9 The dimensionless normal stress distribution $\sigma_y(0,y)/(P/h)$ along the axis of symmetry for (R/h)

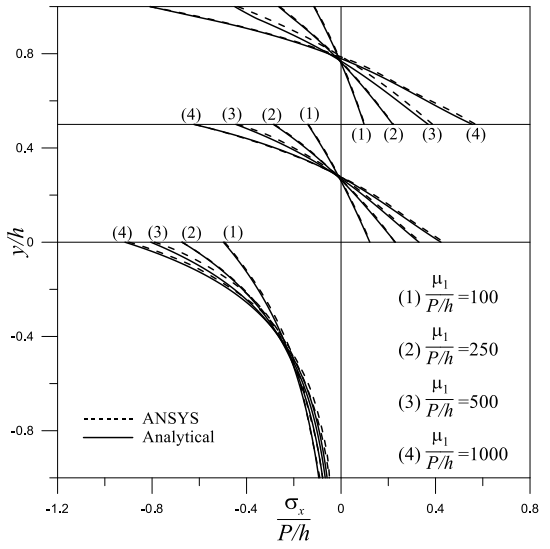

(R/h=500, h_2/h_1=1, μ_2/μ_1=μ_3/μ_2=2, $\rho_1 g h h_1/P$=0.2, ρ_2/ρ_1=1)

Fig. 10 The dimensionless normal stress distribution $\sigma_x(0,y)/(P/h)$ along the axis of symmetry for $\mu_1/(P/h)$

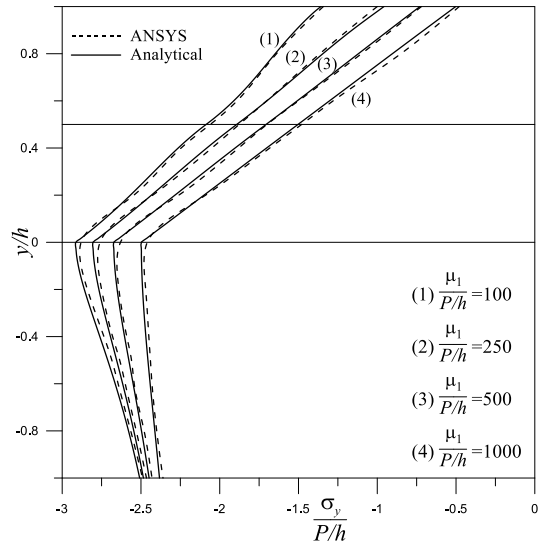

(R/h=500, h_2/h_1=1, μ_2/μ_1=μ_3/μ_2=2, $\rho_1 g h h_1/P$=1, ρ_2/ρ_1=1)

Fig. 11 The dimensionless normal stress distribution $\sigma_y(0,y)/(P/h)$ along the axis of symmetry for $\mu_1/(P/h)$

$\mu_1/(P/h)$ are shown in Figs. 10-11. As it can be seen in the figures, $\sigma_x(0,y)/(P/h)$ and $\sigma_y(0,y)/(P/h)$increase with increasing $\mu_1/(P/h)$. Furthermore, when Figs. 8 and 10 are examined, it can be observed that tension and compression zones occur for each layer. Similar to beams under

bending, the upper regions of layers are in compression and the lower regions are in tension. For semi-infinite plane, the dimensionless normal stress $\sigma_x(0,y)/(P/h)$ is in compression everywhere, takes the maximum value on contact surface (lower layer-semi infinite plane), and approaches to zero as getting deeper.

When Figs. 9 and 11 are analyzed, it can be seen that maximum value of $\sigma_y(0,y)/(P/h)$ along the axis of symmetry is obtained on the contact surface (lower layer-semi infinite plane) and it increases for the layers while moving away from the punch (as going deeper). $\sigma_y(0,y)/(P/h)$ dimensionless stresses get the same values on the contact surface of the layers and on the contact surface between semi-infinite plane and lower layer. This result shows that the boundary conditions (23) and (27) given in the definition of the problem are provided. As long as the contact surface between punch and upper layer becomes smaller, the dimensionless normal stress $\sigma_y(0,y)/(P/h)$ increases rapidly as getting closer to the contact region due to a singularity similar to concentrated load singularity. For the semi-infinite plane, $\sigma_y(0,y)/(P/h)$ approaches to zero as getting deeper since its body force is neglected.

5. Conclusions

The main objective of this study is to present comparison between analytical and FEM calculations of a continuous contact problem. In the paper, the contact areas, contact stress distributions under rigid circular punch and normal stress distributions (σ_x and σ_y) along the axis of symmetry are calculated by using analytical method and finite element method. Finally, these two solutions are compared with each other. The conclusions drawn from the study can be presented as below:

• The results obtained from both solutions show that the contact areas, the contact stresses and the normal stresses are influenced by the compressive resultant force, the relative elastic constants of the layers and semi-infinite plane, the radius of rigid punch and load ratio.

• The contact stresses and the normal stresses obtained from finite element analysis (FEA) provide boundary conditions of the problem as well as analytical results. When FEA results for contact areas are compared with analytical results, it can be clearly seen that contact areas obtained from FEA are very close to analytical results and a good agreement between two methods is observed during this comparison, disagree by 0.03-1.61%.

• Contact stress distribution under rigid punch is symmetrical, its maximum value occurs at x=0 and its value is zero at the end points of contact ($-a$,$+a$). When the analytical and FEA results are compared to each other, it can be clearly seen that there is a good agreement between two methods.

• When dimensionless normal stress $\sigma_x(0,y)/(P/h)$ along the axis of symmetry is examined, it can be seen that tension and compression zones occur for each layer. Similar to beams under bending, the upper regions of layers are in compression and the lower regions are in tension. For semi-infinite plane, the dimensionless normal stress $\sigma_x(0,y)/(P/h)$ is in compression everywhere, takes the maximum value on contact surface (lower layer-semi infinite plane), and approaches to zero as getting deeper.

• When dimensionless normal stress $\sigma_y(0,y)/(P/h)$ along the axis of symmetry is analyzed, it can be clearly seen that maximum value of $\sigma_y(0,y)/(P/h)$ along the axis of symmetry is obtained on the contact surface (lower layer-semi infinite plane) and it increases for the layers while moving away from the punch (as going deeper). Dimensionless normal stresses $\sigma_y(0,y)/(P/h)$get the same

values on the contact surface of the layers and on the contact surface between semi-infinite plane and lower layer. This result shows that the boundary conditions given in the definition of the problem are provided. As long as the contact surface between punch and upper layer becomes smaller, the dimensionless normal stress $\sigma_y(0,y)/(P/h)$ increases rapidly as getting closer to the contact region due to a singularity similar to concentrated load singularity. For the semi-infinite plane, $\sigma_y(0,y)/(P/h)$ approaches to zero as getting deeper since its body force is neglected.

• The dimensionless normal stresses $\sigma_x(0,y)/(P/h)$ and $\sigma_y(0,y)/(P/h)$ decrease with increasing of R/h. Also, they increase with increasing of $\mu_1/(P/h)$.

• Finally, the presented results show that finite element analysis (FEA) carried out in ANSYS software gives results which are in very good agreement with the analytical solution.

References

Adams, G.G. (1978), "An elastic strip pressed against an elastic half plane by a steadily moving force", *J. Appl. Mech.*, **45**(1), 89-94.

Adıbelli, H., Comez, I. and Erdol, R. (2013), "Receding contact problem for a coated layer and a half-plane loaded by a rigid cylindrical stamp", *Arch. Mech.*, **65**(3), 219-236.

Alexandrov, V.M. (1970), "On plane contact problems of the theory of elasticity in the presence of adhesion or friction", *J. Appl. Math. Mech.*, **34**(2), 232-243.

ANSYS (2008), Swanson Analysis System, USA.

Argatov, I. (2013), "Contact problem for a thin elastic layer with variable thickness: application to sensitivity analysis of articular contact mechanics", *Appl. Math. Model.*, **37**(18-19), 8383-8393.

Birinci, A. and Erdol, R. (2001), "Continuous and discontinuous contact problem for a layered composite resting on simple supports", *Struct. Eng. Mech.*, **12**(1), 17-34.

Birinci, A. and Erdol, R. (2003), "A frictionless contact problem for two elastic layers supported by a winkler foundation", *Struct. Eng. Mech.*, **15**(3), 331-344.

Brizmer, V., Kligerman, Y. and Etsion, I. (2006), "The effect of contact conditions and material properties on the elasticity terminus of a spherical contact", *Int. J. Solid. Struct.*, **43**, 5736-5749.

Cakiroglu, F., Cakiroglu, M. and Erdol, R. (2001), "Contact problems for two elastic layers resting on elastic half-plane", *J. Eng. Mech.*, ASCE, **127**(2), 113-118.

Chan, S.K. and Tuba, I.S. (1971), "A finite element method for contact problems of solid bodies-1: theory and validation", *Int. J. Mech. Sci.*, **13**(7), 615-625.

Comez, I. and Erdol, R. (2013), "Frictional contact problem of a rigid stamp and an elastic layer bonded to a homogeneous substrate", *Arch. Appl. Mech.*, **83**(1), 15-24.

Dag, S., Guler, M.A., Yildirim, B. and Ozatag, A.C. (2009), "Sliding frictional contact between a rigid punch and a laterally graded elastic medium", *Int. J. Solid. Struct.*, **46**(22-23), 4038-4053.

Dempsey, J.P., Zhao, Z.G., Minnetyan, L. and Li, H. (1990), "Plane contact of an elastic layer supported by a winkler foundation", *J. Appl. Mech.*, **57**(4), 974-980.

Dini, D. and Nowell, D. (2004), "Flat and rounded fretting contact problems incorporating elastic layers", *Int. J. Mech. Sci.*, **46**(11), 1635-1657.

El-Borgi, S., Abdelmoula, R. and Keer, L. (2006), "A receding contact plane problem between a functionally graded layer and a homogeneous substrate", *Int. J. Solid. Struct.*, **43**(3-4), 658-674.

Erdogan, F. and Gupta, G. (1972), "On the numerical solutions of singular integral equations", *Q. Appl. Math.*, **29**, 525-534.

Etsion, I., Kligerman, Y. and Kadin, Y. (2005), "Unloading of an elastic-plastic loaded spherical contact", *Int. J. Solid. Struct.*, **42**, 3716-3729.

Francavilla, A. and Zienkiewicz, O.C. (1975), "A note on numerical computation of elastic contact problems", *Int. J. Numer. Meth. Eng.*, **9**(4), 913-924.

Galin, L.A. (2008), *Contact Problems*, Springer.
Garrido, J.A., Foces, A. and Paris, F. (1991), "BEM applied to receding contact problems with friction", *Math. Comput. Model.*, **15**(3-5), 143-153.
Garrido, J.A. and Lorenzana, A. (1998), "Receding contact problem involving large displacements using the BEM", *Eng. Anal. Bound. Elem.*, **21**(4), 295-303.
Gecit, M.R. (1986), "Axisymmetric contact problem for a semi-infinite cylinder and a half space", *Int. J. Eng. Sci.*, **24**(8), 1245-1256.
Gun, H. and Gao, X.W. (2014), "Analysis of frictional contact problems for functionally graded materials using BEM", *Eng. Anal. Bound. Elem.*, **38**, 1-7.
Jing, H.S. and Liao, M.L. (1990), "An improved finite element scheme for elastic contact problems with friction", *Comput. Struct.*, **35**(5), 571-578.
Kahya, V., Ozsahin, T.S., Birinci, A. and Erdol, R. (2007), "A receding contact problem for an anisotropic elastic medium consisting of a layer and a half plane", *Int. J. Solid. Struct.*, **44**(17), 5695-5710.
Kumar, N. and Dasgupta, A. (2013), "On the contact problem of an inflated spherical hyperelastic membrane", *Int. J. Nonlin. Mech.*, **57**, 130-139.
Li, X.Y., Zheng, R.F. and Chen, W.Q. (2014), "Fundamental solutions to contact problems of a magneto-electro-elastic half-space indented by a semi-infinite punch", *Int. J. Solid. Struct.*, **51**(1), 164-178.
Liao, X. and Wang, G.G. (2007), "Non-linear dimensional variation analysis for sheet metal assemblies by contact modeling", *Finite Elem. Anal. Des.*, **44**(1-2), 34-44.
Long, J.M. and Wang, G.F. (2013), "Effects of surface tension on axisymmetric hertzian contact problem", *Mech. Mater.*, **56**, 65-70.
Ma, L.F. and Korsunsky, A.M. (2004), "Fundamental formulation for frictional contact problems of coated systems", *Int. J. Solid. Struct.*, **41**(11-12), 2837-2854.
Nowell, D. and Hills, D.A. (1988), "Contact problems incorporating elastic layers", *Int. J. Solid. Struct.*, **24**(1), 105-115.
Oysu, C. (2007), "Finite element and boundary element contact stress analysis with remeshing technique", *Appl. Math. Model.*, **31**(12), 2744-2753.
Porter, M.I. and Hills, D.A. (2002), "Note on the complete contact between a flat rigid punch and an elastic layer attached to a dissimilar substrate", *Int. J. Mech. Sci.*, **44**(3), 509-520.
Ratwani, M. and Erdogan, F. (1973), "On the plane contact problem for a frictionless elastic layer", *Int. J. Solid. Struct.*, **9**(8), 921-936.
Rhimi, M., El-Borgi, S. and Lajnef, N. (2011), "A double receding contact axisymmetric problem between a functionally graded layer and a homogeneous substrate", *Mech. Mater.*, **43**(12), 787-798.
Rončević, B. and Siminiati, D. (2010), "Two dimensional receding contact analysis with nx nastran", *Adv. Eng.*, **4**, 69-74.
Satish Kumar, K., Dattaguru, B., Ramamurthy, T.S. and Raju, K.N. (1996), "Elastoplastic contact stress analysis of joints subjected to cyclic loading", *Comput. Struct.*, **60**(6), 1067-1077.
Soldatenkov, I.A. (2013), "The periodic contact problem of the plane theory of elasticity. Taking friction, wear and adhesion into account", *Pmm. J. Appl. Math. Mech.*, **77**(2), 245-255.
Weitsman, Y. (1972), "A tensionless contact between a beam and an elastic half space", *Int. J. Eng. Sci.*, **10**(1), 73-81.
Yaylaci, M. and Birinci, A. (2013), "The receding contact problem of two elastic layers supported by two elastic quarter planes", *Struct. Eng. Mech.*, **48**(2), 241-255.
Zhang, W.M. and Meng, G. (2006), "Numerical simulation of sliding wear between the rotor bushing and ground plane in micromotors", *Sens. Actuat. A Phys.*, **126**(1), 15-24.

Appendix

Expression of the kernel $k(x,t)$ appearing in (32) is given below.

$$k(x,t)=\frac{1}{h}\int_0^{\infty}\left\{\frac{1}{\Delta^{**}}[[e^{-5z-4z\xi}(-4z^2\xi^2e^{z+2z\xi}(m_1(1+\chi_1)(e^{4z}-2e^{2z+2z\xi}+e^{4z\xi})+4e^{2z+2z\xi}\right.$$
$$(1+\chi_2))(1+\chi_3)-4z\xi(1+\chi_2)e^{z+2z\xi}(m_2(-m_1(1+\chi_1)(e^{4z}-2e^{2z+2z\xi}+e^{4z\xi})$$
$$+(1+\chi_2)e^{2z}(1-2e^{2z\xi}+e^{4z\xi}))+(-e^{2z}+e^{4z\xi}-e^{4z}+e^{2z+4z\xi}-4ze^{2z+2z\xi})$$
$$(1+\chi_3)+e^{z}(m_1(1+\chi_1)(e^{4z}-2e^{2z+2z\xi}+e^{4z\xi})(m_2(1+\chi_2)(-1+e^{4z\xi})+(1+$$
$$\chi_3)(1-2e^{2z\xi}+e^{4z\xi}))+(1+\chi_2)(e^{4z}-e^{4z\xi}+4ze^{2z+2z\xi})((m_2(1+\chi_2)(1-\ 2e^{2z\xi}$$
$$\left.+e^{4z\xi})+(1+\chi_3)(-1+e^{4z\xi})))]-1\right\}\sin\left[(t-x)\frac{z}{h}\right] \qquad \text{(A.1)}$$

where

$$\Delta^{**}=e^{-4z-4z\xi}[16e^{2z+4z\xi}z^3\xi^3(-(1+\chi_2)+m_1(1+\chi_1))(1+\chi_3)-(-e^{4z}+e^{4z\xi}-4ze^{2z+2z\xi})$$
$$m_1(1+\chi_1)((-1+e^{4z\xi})m_2(1+\chi_2)+(1-2e^{2z\xi}+e^{4z\xi})(1+\chi_3))+(e^{4z}+e^{4z\xi}-2e^{2z+2z\xi})$$
$$(1+2z^2))(1+\chi_2)((1-2e^{2z\xi}+e^{4z\xi})m_2(1+\chi_2)+(-1+e^{4z\xi})(1+\chi_3))-4z^2(e^{2z+4z\xi}(1+$$
$$\chi_2)((1-2e^{2z\xi}+e^{4z\xi})m_2(1+\chi_2)+(-1+e^{4z\xi}-8ze^{2z\xi})(1+\chi_3))-m_1(1+\chi_1)(-4e^{2z+4z\xi}$$
$$m_2(1+\chi_2)+(e^{6z\xi}-e^{4z+2z\xi}-4ze^{2z+4z\xi})(1+\chi_3)))-4z\xi e^{2z\xi}(m_1(1+\chi_1)((-e^{4z}+e^{4z\xi}-$$
$$e^{2z}-4ze^{2z+2z\xi}+e^{2z+4z\xi})m_2(1+\chi_2)+(e^{2z}(1-2e^{2z\xi}+e^{4z\xi})(1+\chi_3))-(1+\chi_2)(2e^{2z}$$
$$(1-2e^{2z\xi}+e^{4z\xi})m_2z(1+\chi_2)+(e^{4z}+e^{4z\xi}-2ze^{2z}+2ze^{2z+4z}-2e^{2z+2z\xi}(1+2z^2\xi^2))$$
$$(1+\chi_3)))]$$